Maximum Power Point Tracking of Direct-Drive PMSG with High-Efficiency Boost Converter

J. Barsana Banu, M. Balasingh Moses and S. Ganapathy

Abstract This chapter describes the variable speed stand-alone wind power supply system that incorporates permanent magnet synchronous generator, three-phase diode rectifier, and improved dc–dc boost converter with resistive load. Improved dc–dc boost converter controls to concentrate the most extreme power from the accessible wind. In the wind generation system, the power converter efficiency is one of the important considerations realizing the system performance. In those systems, dc-dc step-up converter is broadly utilized for high-conversion system. Considering the converter's expense and efficiency, this chapter mostly concentrates on the outline of an enhanced topology of the boost converter received for high-power stand-alone wind power system. It describes the perturbation and observation maximum power point tracking algorithm. The MPPT algorithm in addition to the dc–dc step-up converter is simulated by MATLAB/Simulink software. The outcomes demonstrate that the dc–dc converter topology can understand the most extreme power point tracking control of the wind turbine.

Keywords DC–DC boost converter · Efficiency · MPPT · Perturb and observe algorithm · WECS

1 Introduction

These days, renewable energy sources are turning into a vital choice to take care of the developing demand of energy such as contamination-free environment and all the while prevent the production of green gas from conventional fossil fuels.

J. Barsana Banu (✉) · M. Balasingh Moses · S. Ganapathy
Electrical and Electronics Engineering, Anna University, Trichy, India
e-mail: barsanajamal@gmail.com

M. Balasingh Moses
e-mail: mosesaut@gmail.com

S. Ganapathy
e-mail: mail2ganpathy@gmail.com

S. SenGupta et al. (eds.), *Advances in Smart Grid and Renewable Energy*,
Lecture Notes in Electrical Engineering 435, https://doi.org/10.1007/978-981-10-4286-7_43

Depending upon the requirements, stand-alone or grid-connected operation is possible also the added advantage of renewable energy sources. Among different sorts of renewable energy sources, wind energy conversion systems have rapidly evolved around the world [1, 2]. Wind turbine, power electronics converter, and controllers are the key factors that are incorporated within the WECS. The wind turbine has the ability to extract power from the wind, which depends upon available wind power. There are two distinct categories based on the rotation axis of wind turbine: horizontal axis wind turbines (HAWTs) and vertical axis wind turbines (VAWTs).

In horizontal axis, the revolution of wind turbine is parallel to the ground, and in vertical axis, the revolution of wind turbines (VAWTs) is opposite to the wind, that is, vertical, and thus dissimilar to the horizontal wind turbines. They can catch winds from any heading beyond the requirement of rotor relocation as the wind bearing alters (Without a special yaw control).

Vertical axis wind turbines were, likewise, utilized as a part of a few applications as they have the favorable position that they don't rely on upon the heading into the wind. It is conceivable to concentrate on control generally less demanding. In any case, there are a few disservices, for example, no self-starting and minimum power coefficient than HAWT. Contrasted with VAWT, HAWT provides maximum efficiency, which is generally connected in the wind energy industry. The HAWT further splits into constant- and variable-speed wind turbines. The fixed-speed wind turbines achieve high efficiency at rated wind speed and possess the benefits that they are uncomplicated and long-lasting, and need lesser development and support cost. In any case, their operation speed is fixed and cannot be controlled by the variation in the wind speed, which outcomes minimum transformation efficiency contrasted with the variable-speed wind turbines.

These days, the vast majority of the wind turbines connected in industry are variable-speed wind turbines to build its energy capture at different wind speeds. Among various types of variable speed WECSs, three sorts are most generally connected to industries: DFIG (double-fed induction generator), SCIG (squirrel-cage induction generator), and WRSG (wound rotor synchronous generator) with geared or gearless or PMSG (permanent magnet synchronous generator) WECSs with full-capacity power converters.

The performances of different topologies of generator–converter combinations of WECS with distinct control algorithms are compared in [3]. With the approach of high-power thickness permanent magnets, the generator is manufactured with a most extreme power thickness contrasted with wound rotor sort bringing about the disposal of extra dc supply for outside excitation, brushes and slip rings gathering. Contrasted with induction generator (IG), PMSG does not require capacitors for excitation and voltage builds up. For small-scale installations, the use of PMSG is more useful on account of its minimized size and high-power density, not a requirement for gearbox.

WECS based on the permanent magnet synchronous generator was investigated in recent researches [4, 5]. Another major benefit of WECS has made an effective move from small stand-alone areas to satisfy consumer demand to high

grid-connected networks. Depending upon the requirement, the grid provides real power to the loads or absorbs the abundance power from the site when accessible. However, significant literature is available on stand-alone power generation with PMSG [6, 7]. The stand-alone system should, consequently, have few methods of reserving energy. It can be utilized afterward to contribute the demand for the period of low or nil output power. Several control strategies and algorithm for stand-alone WECS are developed for variable wind speed, and the load is described in [8, 9]. Most of WECS are projected for grid-connected systems [10]. In [11], an effortless control method is presented for finest extraction of power from grid-tied PMSG-VS wind energy conversion. It utilizes sensor less maximum power point tracking algorithm but with lagging power factor.

In [12], sliding mode (SM) evaluation of DTC is investigated to maximize the extracted power at unity power factor. The execution of WECS has been shown under fluctuating wind circumstances. At that point, the networks not only obtain the most extreme power but also keep up the unity power factor output voltage at fixed frequency. MPPT procedure is employed for obtaining the most extreme power available in the wind. The principal MPPT strategies are as follows: tip-speed ratio (TSR), optimum relation based (ORB) (power vs. speed and power vs. torque), and perturb and observe (P&O) strategies.

Various MPPT techniques are described in [13]. The power electronic converter integration plays a vital role in understanding the maximum power point tracking (MPPT) process [14]. The methodology of a converter in view of a 3Φ rectifier with the boost converter is more appropriate for small wind energy system requirements in view of its minimum price and high consistency [15], and MPPT estimation with modified perturb and observe algorithm is projected to fulfill an optimization of the MPPT in the quickly changing wind speed.

This chapter focuses the stand-alone wind power supply system with improved power electronic boost converter control to track the most extreme power from the accessible wind in all directions as shown in Fig. 1. The detailed modeling of wind turbine and permanent magnet synchronous generator is described in Sects. 2 and 3. Uncontrolled rectifier and proposed boost converter are explained in Sects. 4 and 5. MPPT algorithm and its implementation are described in Sect. 6. Simulation analyses are carried out in Sect. 7. Finally, conclusions are drawn in Sect. 8.

2 Modeling of Wind Turbine

The power obtained from the wind has the accompanying expression:

$$P_w = \frac{1}{2} q \pi R^2 V_w^3 C_p \tag{1}$$

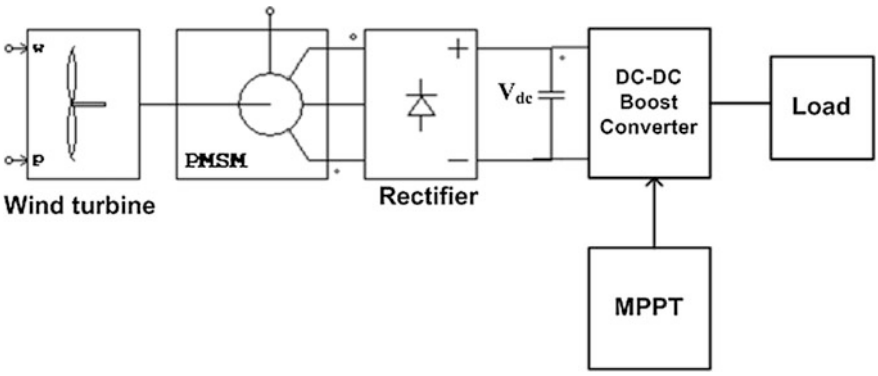

Fig. 1 Proposed system arrangement

R Turbine sweep (radius) (m)
q Thickness of the air (kg/m^3)
V_w Velocity of the wind (m/s)
C_p Turbine power coefficient

The wind turbine torque can be expressed as follows:

$$T_w = \frac{P_w}{\Omega_m} = \frac{1}{2}\rho\pi R^2 \frac{V_w}{\Omega_m} C_p \tag{2}$$

Ω_m Pivot velocity of the turbine (rad/s). The power coefficient can be communicated as follows:

$$C_p = 0.5176\left(\frac{116}{\lambda_i} - 0.4\beta - 5\right)e^{\frac{-21}{\lambda_1}} + 0.0068\lambda \tag{3}$$

$$\frac{1}{\lambda_i} = \frac{1}{\lambda + 0.08\beta} - \frac{0.055}{\beta^3 + 1} \tag{4}$$

where β is the angle of the blades (rad) and λ is the tip-speed ratio (TSR) which is represented by:

$$\lambda = \frac{R\Omega_m}{V_w} \tag{5}$$

It is observed that the TSR is optimum ($K\Omega_{\text{mopt}}$) at maximum power coefficient $C_{P\text{max}}$. Hence, the wind power extraction is higher. At this condition, optimum power is attained by applying λ in (1)

$$P_{w\max} = K\Omega_{\text{mopt}}^3 \tag{6}$$

Equation (6) should be utilized to understand the MPPT examination.

$$K = \frac{\frac{1}{2}\rho\pi R^5 C_{p\max}}{\lambda_{\text{opt}}^3} \tag{7}$$

where K is the power gain at maximum power and Ω_{mopt} is an ideal turn speed compared to a particular wind speed.

3 PMSG Modeling

The modeling of PMSG is represented by d–q reference frame by the following:

$$V_d = R_s i_d + L_d \frac{\mathrm{d}i_d}{\mathrm{d}t} - w_e L_q i_q \tag{8}$$

$$V_q = R_s i_q + L_q \frac{\mathrm{d}i_q}{\mathrm{d}t} - w_e L_d i_d + w_e \Phi_m \tag{9}$$

where V_d and V_q are d and q components of stator voltages (V); i_d and i_q are stator current (A) of the d and q components; R_s is the resistance in the stator (ohms); L_d and L_q are the d- and q-axis machine inductances (H); ω_e is the electric speed (rad/s); and φ_m is the flux (wb).

The electrical torque is obtained from the accompanied equation:

$$T_e = \frac{3}{2} p\left\{\Phi_m i_q + (L_d - L_q) i_d i_q\right\} \tag{10}$$

where p is the pole pairs. The dynamics of the machine rotor is given as follows:

$$T_m - T_e = B w_r + J \frac{\mathrm{d}w_r}{\mathrm{d}t} \tag{11}$$

where B is the rotor friction (kg m^2/s), J is the rotor inertia (kg m^2), ω_r is rotor speed (rad/s), and T_m is the mechanical torque created by wind (Nm).

For simplification, assume ($L_d = L_q = 0$), the d reference current is zero ($i_{\text{d}}^* = 0$), and hence, the product term ($L_d - L_q$) $i_d i_q$ is negligible.

4 Diode Rectifier

The 3Φ full-wave bridge rectifier can be connected directly to the three-phase source to convert the ac output voltage from the PMSG to the rectified dc. The average dc output voltage across the rectifier is as follows:

$$V_{\mathrm{dc}} = \left(3\sqrt{2}/\pi\right) V_L \tag{12}$$

where V_{dc} is dc or average output voltage across the rectifier, and V_L is the ac line voltage from PMSG.

5 DC–DC Boost Converter

The unregulated dc voltage from the diode rectifier is given as input to the improved boost converter. The rectifier output voltage will fluctuate due to variations in wind speed. Improved step-up converter is needed to obtain the regulated dc output voltage and also to understand the MPPT process. A single-control switch S is desirable due to its low expense and robust control. The resistive burden R_{L} associated with step-up converter is expected to acquire the power from WECS. The boost converter output voltage is obtained as follows:

$$\frac{V_0}{V_{\mathrm{dc}}} = \frac{1}{1-K} = \frac{I_0}{I_{\mathrm{dc}}} \tag{13}$$

The MPPT computation utilizes the dc voltage and current acquired from the rectifier to regulate the duty cycle K.

6 MPPT Algorithm

The MPPT computation processes the optimum speed for the most extreme power point utilizing data on direction and magnitude of output power variation owing to the variation in grasp speed. The stream diagram for MPPT is shown in Fig. 2. It depicts the step-by-step execution of proposed MPPT procedure. The controller operation is clarified underneath. The active power $P_0(k)$ is calculated, and if the distinction between its values at present and past examining moment, $\Delta P_0(k)$ is within a predefined minimum and maximum power limits P_{min} and P_{max} correspondingly; then, no action is made; still, if the distinction is outside this extent, at that point, certain important control move is made. The control activity made relies on the direction and magnitude of power variation because of the adjustment to the grasp speed.

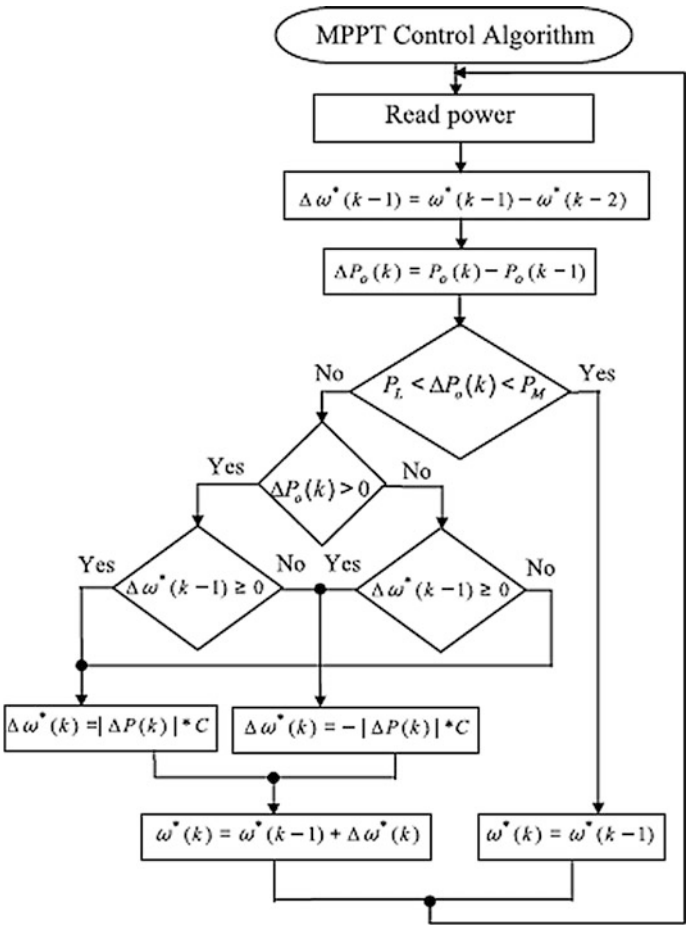

Fig. 2 Flowchart for the proposed MPPT algorithm

(i) On the off chance that the power in the present testing moment is observed to be higher, i.e., $\Delta P_0(k) > 0$ either because of an expansion in grasp speed or grasp speed staying unaltered in the past examining moment, i.e. $\Delta\omega^*(k-1) \geq 0$, after that the grasp speed is increased.

(ii) If the power in current testing moment is observed to be higher, i.e., $\Delta P_0(k) > 0$, because of diminution in the grasp speed over the past examining moment, i.e., $\Delta\omega^*(k-1) < 0$, after that the reference speed is reduced.

(iii) In addition, if the power diminishing in the current inspecting moment is observed, i.e., either because of a steady or expanded grasp speed over the past examining moment, i.e., $\Delta\omega^*(k-1) \geq 0$, at that moment grasp speed is minimized.

(iv) At long last, if the power in current testing moment is observed to be diminished, i.e., $\Delta P_0(k) < 0$, because of an abatement in grasp velocity in the past examining moment, i.e. $\Delta\omega^*(k-1) < 0$, the grasp speed is incremented.

The extent of variation, assuming any, in the reference velocity in a control sequence is chosen by the result of extent of power error $\Delta P_0(k)$ and C. The quality C is chosen by the rate as the wind speed. All along the most extreme power point tracking process handles the item said above reductions gradually lastly equivalents to zero at the crest power point.

To have the incredible following ability at all wind ranges, the estimation of C ought to fluctuate the variation at the adjustment in the wind velocity. If the wind rate is not ascertained, rotor velocity is used to set its regard. After that, at lower wind speed, power varies with speed deviation and the rate of C is higher; then, the speed increases as C decreases. In the proposed chapter, a number of simulations are carried out with distinct inputs to find out the above-mentioned values which indicate the excellent outcomes.

7 Results and Discussions

Wind turbine with MPPT control of the improved boost converter is completed utilizing MATLAB simulation software to assess the feasibility of the presented configuration. Simulink model of wind-driven PMSG step-up converter is shown in Fig. 3.

The sub-blocks of wind turbine and MPPT controller are shown in Fig. 3. The perturb and observe MPPT controller initially measures the power from the wind and compares the power in the present state and in the previous state. Based on the ratio of difference in the power, the duty ratio of the boost converter switch can be

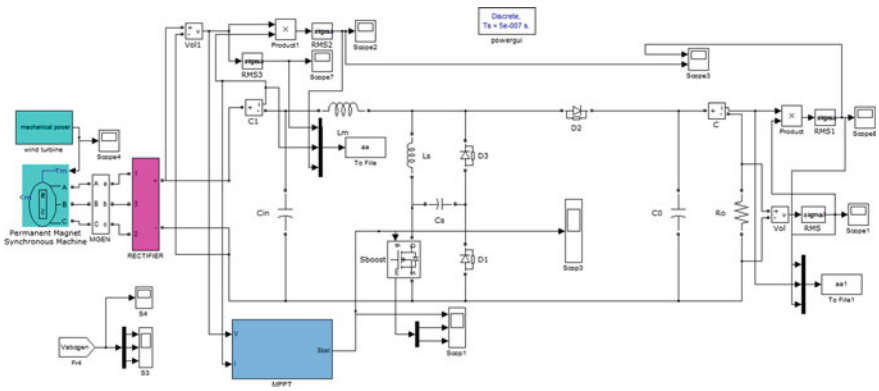

Fig. 3 Simulink model

perturbed at each second, and the different characteristics of the wind turbine are shown in Fig. 4.

The wind turbine operating for 15 and 17 m/s is considered and measures the rectifier outputs and the improved boost converter outputs. Figures 5a and 6a depict the dc waveforms of the uncontrolled bridge rectifier for 15 and 17 m/s wind speeds. Figures 5b and 6b represent the converter waveforms, respectively, by considering the wind speed at 15 and 17 m/s at the phase angle of 0°. The proposed boost converter receives input from the uncontrolled bride rectifier then this boost converter step up this uncontrolled dc outputs in order to be controlled dc voltage, current and power, double the input given and achieves the high converter efficiency up to 97%. If the wind speed increases from 15 to 17 m/s, the output voltage and power also increased as shown in Figs. 5 and 6.

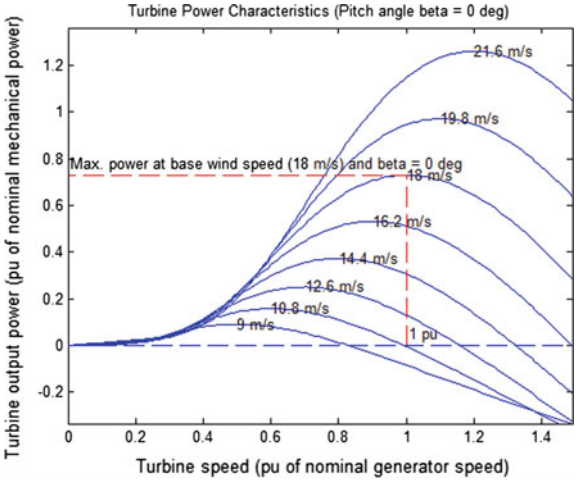

Fig. 4 Characteristics of the wind turbine

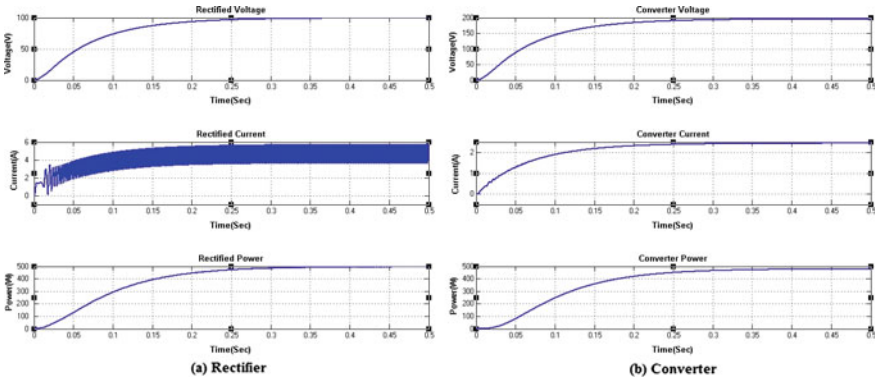

Fig. 5 O/P voltage, current, and power at 15-m/s wind speed. **a** Rectifier and **b** converter

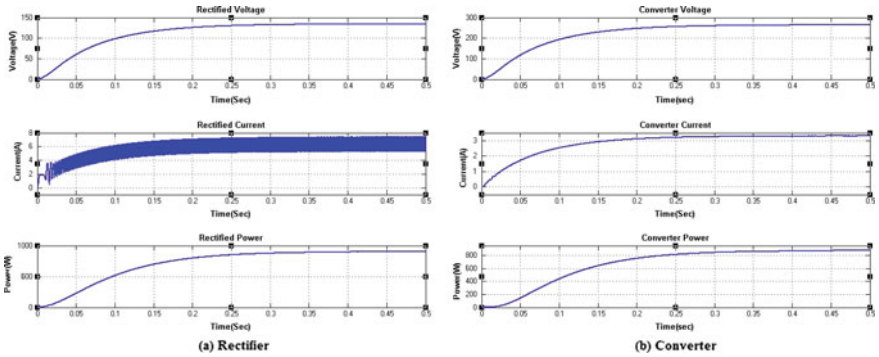

Fig. 6 O/P voltage, current, and power at 17-m/s wind speed. **a** Rectifier and **b** converter

8 Conclusion

In this chapter, the wind-driven PMSG with high-efficiency dc–dc step-up converter is described. The perturb and observe algorithm works efficiently for the proposed boost converter circuit. The simulation results for two different wind speeds are compared and show that the proposed boost converter achieves high efficiency with maximum power point tracking. The topology and control strategy of the proposed converter provide a valid solution for stand-alone wind turbine applications.

References

1. Babu, N.R., Arulmozhivarman, P.: Wind energy conversion systems-a technical review. J. Eng. Sci. Technol. **8**(4), 493–507 (2013)
2. Kekezoglu, B., Tanrioven, M., Erduman, A.: A new wind turbine concept: design and implementation. Acta Polytech. Hung. **12**(3), 199–211 (2015)
3. Baroudi, J.A., Dinavahi, V., Knight, A.M.: A review of power converter topologies for wind generators. Renewable Energy. **32**(14), 2369–2385 (2007)
4. Messaoud, M., Abdessamed, R.: Modeling and optimization of wind turbine driving permanent magnet synchronous generator. Jordan J. Mech. Ind. Eng. **5**(6), 489–494 (2011)
5. Wu, Z., Dou, X., Chu, J., Hu, M.: Operation and control of a direct-driven PMSG-based wind turbine system with an auxiliary parallel grid-side converter. Energies **6**(7), 3405–3421 (2013)
6. Vlad, C., Bratcu, A.: Munteanu. I., Epure, S.: Real-time replication of a stand-alone wind energy conversion system: error analysis. Int. J. Electr. Power Energy Syst. **55**, 562–571 (2014)
7. Singh, B., Sharma, S.: Stand-alone wind energy conversion system with an asynchronous generator. J. Power Electron. **10**(5), 538–554 (2010)
8. Hussein, M.M., Senjyu, T., Orabi, M., Wahab, M.A., Hamada, M.M.: Control of a stand-alone variable speed wind energy supply system. Applied Sciences. **3**(2), 437–456 (2013)

9. Lopez, M., Vannier, J.C.: Stand-alone wind energy conversion system with maximum power transfer control. Ingeniare. Revistachilena de ingenieria **17**(3), 329–336 (2009)
10. Linus, R.M., Damodharan, P.: Maximum power point tracking method using a modified perturb and observe algorithm for grid connected wind energy conversion systems. IET Renew. Power Gener. **9**(6), 682–689 (2015)
11. Linus, R.M., Damodharan, P.: Wind Velocity Sensorless Maximum Power Point Tracking Algorithm in Grid-connected Wind Energy Conversion System. Electric Power Compon. Systems. **43**(15), 1761–1770 (2015)
12. Errami, Y., Maaroufi, M., Ouassaid, M.: Maximum power point tracking of a wind power system based on the PMSG using sliding mode direct torque control, In: International Renewable and Sustainable Energy Conference (IRSEC), Ouarzazate, pp. 218–223 (2013)
13. Abdullah, M.A., Yatim, A.H.M., Tan, C.W., Saidur, R.: A review of maximum power point tracking algorithms for wind energy systems. Renew. Sustain. Energy Rev. **16**(5), 3220–3227 (2012)
14. Li, P., Li, D.Y., Wang, L., Cai, W.C., Song, Y.D.: Maximum power point tracking for wind power systems with an improved control and extremum seeking strategy. Int. trans. electr. energy syst. **24**(5), 623–637 (2014)
15. Daili, Y., Gaubert, J.P., Rahmani, L.: Implementation of a new maximum power point tracking control strategy for small wind energy conversion systems without mechanical sensors. Energy Convers. Manag. **97**, 298–306 (2015)